Research Article

Molecular cloning and tissue expression analysis of tumor necrosis factor (TNF) gene from *Macrobrachium rosenbergii* in response to pathogen infections

Phornchatra Suksangiamkul[1], Chanitcha Choolert[1], Natchaphon Ngueanngam[2], Phongthana Pasookhush[3], Akapon Vaniksampanna[4], Siwaporn Longyant[1,5] and Parin Chaivisuthangkura[1,5*]
_____

ABSTRACT

Tumor necrosis factor (TNF) is a cytokine that plays essential roles in various physiological pathways, including inflammation and immune responses to microbial infections. Therefore, in this study, we isolated and characterized the full-length TNF gene in *Macrobrachium rosenbergii* (*MrTNF*) and investigated the expression of *MrTNF* against *Aeromonas hydrophila* and *Macrobrachium rosenbergii* nodavirus (*Mr*NV) infections. The full-length cDNA of *MrTNF* had 1830 base pairs (bp), consisting of a 5′ untranslated region (5′-UTR) of 396 bp and a 3′-UTR of 54 bp. *MrTNF* contained an open reading frame (ORF) of 1380 bp, encoding 459 amino acid residues. The structural analysis of *Mr*TNF revealed a transmembrane domain from positions 21 to 43 and a conserved TNF domain from positions 324 to 446. The *Mr*TNF protein exhibited a high identity of 91.88% compared with *Mn*TNF from *Macrobrachium nipponense*. The phylogenetic tree analysis revealed that *Mr*TNF was closely related to *Mn*TNF from *M. nipponense*. The expression level of *MrTNF* mRNA in healthy prawns exhibited high expression in the intestine, muscle, and stomach. *MrTNF* was significantly up-regulated in hemocytes, muscle, intestine, and stomach upon *A. hydrophila* infection. Furthermore, *MrTNF* in muscle, gills, and hepatopancreas was significantly up-regulated upon *Mr*NV challenge. Molecular docking study indicated that *Mr*TNF may interact with the protruding (P)-domain of *Mr*NV triggering a response in the innate immune system of prawns after viral infection. These findings suggest that *MrTNF* plays a crucial role in the innate immune system of freshwater crustaceans, particularly in response to Gram-negative bacteria and viral infections.

_____
[1] Department of Biology, Faculty of Science, Srinakharinwirot University, Bangkok 10110, Thailand
[2] Department of Chemistry, Faculty of Science, Srinakharinwirot University, Bangkok 10110, Thailand
[3] Division of Medical Bioinformatics, Research Division, Faculty of Medicine Siriraj Hospital, Mahidol University, Bangkok 10700, Thailand `
[4] Innovative Learning Center, Srinakharinwirot University, Bangkok 10110, Thailand
[5] Center of Excellence for Animal, Plant and Parasite Biotechnology, Srinakharinwirot University, Bangkok 10110, Thailand
*Corresponding author, email: Parin Chaivisuthangkura (parin@g.swu.ac.th)

Introduction

Tumor necrosis factor (TNF) is a crucial protein that regulates various cellular processes in vertebrates, such as inflammation, cell differentiation, proliferation, apoptosis, necrosis, and cell survival [1]. The TNF superfamily (TNFSF) comprises 19 ligands and 29 receptors [2]. The TNF ligands are classified as type II membrane proteins characterized by an intracellular N terminus and an extracellular C terminus containing a TNF homology domain (THD) [3], which allows the ligand to exist in both membrane-bound and soluble forms [4]. TNF binds to specific TNF receptors superfamily (TNFRSF) located on the surface of target cells, initiating a cascade of signaling events that ultimately activate immune responses. In mammals, TNF initiates the activation of the NF-ΚB and activator protein 1 (AP-1) pathways. These pathways play a crucial role in the expression of proinflammatory cytokines, and the mixed lineage kinase domain-like (MLKL) cascade [5].

The first TNFSF member in invertebrates was identified as the TNF ligand, Eiger (ectodysplasin-like cell death trigger), in the fruit fly *Drosophila melanogaster*, which was named *Dm*Eiger [6]. Along with its corresponding TNFRSF member (Wengen), *Dm*Eiger induced an immune response that leads to cell death by activating the c-Jun N-terminal kinase (JNK) pathway in *Drosophila* [7]. The presence of TNFs and their homologs in various invertebrate species have been a topic of research, and several studies have reported the identification of TNF-like proteins in several invertebrates. For example, the mollusk *Haliotis discus discus* [8], Pacific oyster *Crassostrea gigas* [9-11], cuttlefish *Sepiella japonica* [12], and Zhikong scallop *Chlamys farreri* [13, 14], and the sea urchin *Strongylocentrotus purpuratus* [15].

In crustacean, various TNFSF members have been isolated and characterized from different species such as kuruma shrimp *Marsupenaeus japonicas* (*Mj*TNF) [16], whiteleg shrimp *Litopenaeus vannamei* (*Lv*TNFSF, TNF receptors superfamily; *Lv*TNFRSF, and Lipopolysaccharide-induced TNF-alpha factor; *Lv*LITAF) [17], crayfish *Procambarus clarkii* [18], oriental river prawn *Macrobrachium nipponense* (*Mn*TNF) [19], and Chinese mitten crab *Eriocheir sinensis* (*Es*TNFSF and *Es*LITAF) [20, 21]. *Mj*TNF shared approximately 30.7% similarity with *Dm*Eiger. Studies on *Mj*TNF expression revealed that *Mj*TNF increased in response to *Vibrio penaeicida* infection, indicating *Mj*TNF responded to Gram-positive bacterial infection [16]. *Lv*TNFSF was found to be closely related to *Mj*TNF at 89.8% similarity. *Lv*TNFSF expression increased when *L. vannamei* was infected with *Staphylococcus aureus*, WSSV, and *Candida albicans*, suggesting that *Lv*TNFSF was involved in the shrimp immune defense system, against Gram-positive bacteria, viruses, and fungi [17]. In addition, *Mn*TNF from *M. nipponense* shared similarities of 76% and 38% with *Mj*TNF and *Dm*Eiger, respectively. *Mn*TNF expression level was enhanced after *Aeromonas veronii* infection, indicating that a *Mn*TNF was related to the shrimp immune response against Gram-negative bacterial infection [19].

The giant freshwater prawn *Macrobrachium rosenbergii*, is an economically important crustacean species widely cultivated for human consumption in many countries, particularly in Thailand and other Southeast Asian countries, including Bangladesh, Cambodia, Malaysia, Myanmar, Philippines, and Vietnam [22]. However, like other aquatic organisms, *M. rosenbergii* is susceptible to various bacterial, viral, and fungal infections. For example, infection with *Aeromonas hydrophila* causes "Shell disease" or "Black spot disease". In contrast, the presence of *Macrobrachium rosenbergii* nodavirus (*Mr*NV) along with co-infection virus, extra small virus (XSV), leads to a disease known as "White Tail Disease (WTD)" [23]. These

pathogens can result in significant economic losses in the aquaculture industry [24, 25]. Understanding the underlying mechanisms of immune defense against these pathogens will be essential in developing effective disease prevention and control strategies.

The present study isolated and characterized the full-length cDNA of tumor necrosis factor from *M. rosenbergii* (*MrTNF*). The tissue distribution of *MrTNF* from various tissues of healthy *M. rosenbergii* was analyzed. In addition, *MrTNF* expression levels in response to *A. hydrophila* and *Mr*NV infections were examined to investigate its potential role in the immune response. The protein interaction was analyzed with *Mr*TNF and the P-domain of *Mr*NV to observe the mechanism of binding to pathogenic invaders in the host immune system.

Materials and methods

Animals

Healthy giant freshwater prawns *M. rosenbergii* (approximately 1-15 g body weight) were kindly provided from Lukkungsetthi-LST farm, Chachoengsao province, Thailand. Healthy adults *M. rosenbergii* (approximately 45-50 g body weight) were purchased from a local market in Bangkok, Thailand. The prawns were placed into a 1 cubic meter recirculating water tank system (with a maximum of 100 prawns per tank). The tank was half-filled with dechlorinated freshwater, air-pumped, and maintained at a temperature of 25-30°C. The prawns were fed a commercial diet once a day and given a minimum of 7 days to acclimate before the experiments. In addition, the prawns were screened for *Mr*NV and XSV infections using reverse-transcription PCR (RT-PCR) [26].

Bacteria and virus for immune challenge experiment

The gram-negative bacteria *Aeromonas hydrophila* VMARC1234 [27] was prepared for the *A. hydrophila* inoculum. The bacteria were cultured in Tryptic Soy Broth (TSB) and incubated overnight at 37°C on a shaker at 225 rpm. The bacterial culture was collected by centrifugation at 2,000x*g* for 20 mins, and the pellet was resuspended with sterile 2X Phosphate-Buffered Saline (2X PBS; Phosphate buffered saline; 135 mM NaCl, 15 mM sodium phosphate, and pH 7.2). The *A. hydrophila* inoculum was verified by PCR using specific primers, AHH1F and AHH1R (Table 1). The primers were specific to the hemolysin gene with an amplicon size of 130 bp [28] using the Platinum® *Taq* DNA Polymerase (Invitrogen, USA) following the manufacturer's protocol. The PCR product was sequenced and analyzed by blastn for verification. A plasmid containing the hemolysin gene was used as a positive control. The PCR reaction without a DNA template was used as a negative control.

Macrobrachium rosenbergii nodavirus (*Mr*NV) was used for the immune challenge experiment. *Mr*NV inoculum was prepared according to the previously described method [29]. Prawns infected with *Mr*NV were homogenized in TN buffer (20-mM Tris-HCl and 0.4-M NaCl, pH 7.4) at a 10% ratio (w/v) using a sterile homogenizer. Subsequently, the resulting mixture was centrifuged at 11,000x*g* for 20 mins at 4°C and filtered through a 0.45 μm membrane to obtain the *Mr*NV inoculum. The *Mr*NV used in this study was verified by RT-PCR with specific primer, RNA1_FP, and RNA1_RP (Table 1) targeting the *Mr*NV RNA1 gene with an amplicon size of 75 bp [30] using the SuperScript One-Step RT-PCR System (Invitrogen,

USA) following the manufacturer's protocol. The PCR product was sequenced and analyzed by blastn for verification. The RT-PCR reaction without an RNA template was used as a negative control.

Table 1 Primers used in this study.

Primers	Sequence (5′-3′)	Applications
TNF.GSP001	GGGCCTGAAGCTGGTGGGTACCGCTGG	Amplification of the full-length cDNA
TNF.NGSP001	CTCCGCCGCTCTTGTCGC TGTCGTCGC	
TNF.GSP002	CCAGCGGTACCCACCAGCTTCAGGCCC	
TNF.NGSP002	CCTCAGCGGCCATCGTGGTCCCACAGA	
UPM	CTAATACGACTCACTATAGGGCAAGCA GTGGTATCAACGCAGAGT	
UPM short	CTAATACGACTCACTATAGGGC	
TNF.qPCR_F	ATCACCCTGGGACATTTCG	qRT-PCR analysis
TNF.qPCR_R	TCCCAGATTGTCCATCCAAG	
EF1α_F	TGCGCTGTGTTGATTGTAGC	
EF1α_R	ACAATGAGCTGCTTGACACC	
AHH1F	GCCGAGCGCCCAGAAGGTGAGTT	*Aeromonas hydrophila* detection (28)
AHH1R	GAGCGGCTGGATGCGGTTGT	
RNA1_FP	CAACTCGGTATGGAACTCAAGGT	*Macrobrachium rosenbergii* nodavirus detection (30)
NA1_RP	AGGAAATACACGAGCAAGAAAAGTC	

Tissue collections and total RNA extraction

Tissues of healthy *M. rosenbergii* were collected from several organs including gills, hepatopancreas, heart, stomach, intestine, muscle, and hemocytes. To obtain hemocytes, 100 μL of hemolymph was drawn from the ventral sinus using a 1 mL syringe and mixed with a 10 volume (1 mL) of Alsever's solution (0.055% citric acid, 0.8% sodium citrate, 2.05% D-glucose, and 0.42% sodium chloride (w/v)). The mixture was centrifuged at 2,000xg for 10 mins at 4°C, and the pellets were washed twice with 1 volume of Alsever's solution and centrifuged at 2,000xg for 5 mins. Total RNA was extracted from the individual collected tissues using a NucleoSpin® RNA Plus isolation Kit (MACHEREY-NAGEL, Germany) following the manufacturer's protocol. The concentration of total RNA was measured using a NanoDrop Lite Spectrophotometer (Thermo Fisher Scientific, USA). Total RNA was stored at -70°C until use.

Isolation of the full-length MrTNF cDNA

To obtain the full-length cDNA of *MrTNF*, specific primers were designed based on the partial sequence received from our previous *M. rosenbergii* transcriptomic study [31]. To isolate the 5′ and 3′ ends of *MrTNF* cDNA, total RNA extracted from muscle tissue was synthesized separately for 5′ and 3′ RACE-

Ready cDNA using SMARTer® RACE cDNA Amplification kit (Clontech, USA) following the manufacturer's protocol. The full-length cDNA of *MrTNF* was isolated using SeqAmp™ DNA Polymerase (Clontech, USA). For the 5′-RACE PCR, the gene-specific primer TNF.GSP0001 and the universal primer mix (UPM) was performed under the following PCR conditions: 1 cycle at 94 °C for 3 mins; 30 cycles at 94 °C for 30 s, 68°C for 30 s, and 72°C for 3 mins. The nested 5′-RACE PCR was subsequently performed using the second set of gene-specific primer TNF.NGSP0001 and universal primer short (UPM short) under the following PCR conditions: 1 cycle at 94 °C for 3 mins; 30 cycles at 94 °C for 30 s, 65°C for 30 s, and 72°C for 3 mins. For the 3′-RACE PCR, the gene-specific primer TNF.GSP0002 and UPM were used, and the nested 3′-RACE PCR was carried out using gene-specific primers TNF.NGSP0002 and UPM short, with PCR conditions as used for the 5′-end isolation. All primers used in RACE PCR are listed in Table 1.

The nested 5′ and 3′- RACE PCR products were cloned into the pCR Blunt II-TOPO Vector using the Zero Blunt® TOPO® Cloning Kit (Invitrogen, USA) and subsequently transformed into *E. coli* TOP10 using heat shock transformation. The recombinant plasmid of *MrTNF* was extracted using NucleoSpin® Plasmid Kit (MACHEREY-NAGEL, Germany) following the manufacturer's protocol. The resulting plasmids prepared from at least six different bacterial clones were sequenced by Sanger's sequencing. The full-length cDNA of *MrTNF* was obtained by aligning and overlapping the sequences of the 5′ and 3′ cDNA ends. To verify the accuracy of the *MrTNF* sequence, the specific primers upstream of the start codon (5′-GGA GTG AAC GCC CTC CCT TGT-3′) and downstream of the stop codon (5′-GAA GCG CTC AGG TAC CGC TTG TAG-3′) were designed and the cDNA prepared from total RNA was used as a template for PCR amplification that cover the entire coding sequence. The obtained PCR product was directly sequenced and analyzed.

Bioinformatics analysis

The full-length cDNA of *MrTNF* was analyzed using the Basic Local Alignment Search Tool (BLAST) program (https://blast.ncbi.nlm.nih.gov/Blast.cgi). To obtain the deduced amino acids of *MrTNF*, the full-length *MrTNF* cDNA was translated into the *Mr*TNF protein using the ORF Finder program (https://www.ncbi.nlm.nih.gov/orffinder/). The theoretical isoelectric point and molecular mass of the *Mr*TNF protein were calculated using the Compute pI/Mw tool (https://web.expasy.org/compute_pi/). The prediction of the signal peptide and structural domains of *Mr*TNF was conducted using the Simple Modular Architecture Research Tool (SMART) with normal mode analysis (http://smart.embl-heidelberg.de/). To compare *Mr*TNF protein with TNF protein from other species, the pairwise alignment was analyzed using the Ident and Sim webserver (https://www.bioinformatics.org/sms2/ident_sim.html). The multiple sequence alignment of *Mr*TNF and other TNFs was performed using the MUSCLE tool version 3.8 (https://www.ebi. ac.uk/Tools/msa/muscle/). The phylogenetic tree was constructed by Molecular Evolutionary Genetics Analysis (MEGA) software version X (http://www.megasoftware.net/). To study the relationship between *Mr*TNF and TNFs across various crustaceans, invertebrates, and vertebrates, the amino acid sequences of the conserved THD of *Mr*TNF and TNFs from other species were used for the construction of a phylogenetic tree using the neighbor-joining (NJ) method with a p-distance model and 1,000 replicates of bootstrap analysis.

Analysis of MrTNF expression in healthy prawn

To determine the mRNA expression levels of *MrTNF* in various tissues of healthy *M. rosenbergii*, three healthy adult prawns (45-50 g body weight) were selected for sample collection. Total RNA was extracted from various organs, including gills, hepatopancreas, heart, stomach, intestine, muscle, and hemocytes. For cDNA synthesis, total RNA (1 μg total) from each tissue was used as a template using the SensiFAST™ cDNA Synthesis Kit (BioLine, UK). The qPCR reaction was carried out using SensiFAST™ SYBR® No-ROX Kit (BioLine, UK) following the manufacturer's protocol. The qPCR was performed using gene-specific primers, TNF.qPCR_F and TNF.qPCR_R (Table 1). The elongation factor 1 alpha (EF1α) gene was used as an internal control gene. The cycling conditions involved an initial step at 95°C for 2 mins, followed by 40 cycles of 95°C for 5s, 60°C for 10s, and 72°C for 10s. The experiment was performed in triplicate. The relative expression of *MrTNF* in different tissues was determined using the $2^{-\Delta\Delta CT}$ method [32] with normalization to the EF1α gene. The results were presented as mean ± SD. The data were analyzed by One-way analysis of variance (ANOVA) with the Post Hoc Tukey test using IBM SPSS Statistics (Version 25). Statistically significant differences were identified at $p<0.05$.

Immune challenge with A. hydrophila

The *A.hydrophila* challenge experiment was conducted based on the pathogenesis timeline of the prawn in response to the bacterial infection [33]. We collected prawn samples at seven time-point, including 0, 3, 6, 12, 24, 36, and 48 hours post-injection (hpi), and the experiment was performed according to our previous studies [34-36]. Briefly, the healthy *M. rosenbergii* (10-15 g body weight) were divided into two groups: an *A. hydrophila*-challenged group, and a control group, each consisting of 21 individual prawns per 100-liter plastic tank. For the *A. hydrophila*-challenged group, prawns were intramuscularly injected at the third abdominal segment using a 1 mL syringe (0.33 x 13 mm) with 100 μL of *A. hydrophila* at $2x10^3$ CFU/μL ($2x10^4$ CFU/g weight). In comparison, the control group was injected with 100 μL of sterile 2X PBS. Target organs, including hemocytes, muscle, intestine, and stomach, were collected from each group (3 prawns per timepoint) at 0, 3, 6, 12, 24, 36, and 48 hpi.

The expression of *MrTNF* in each group was determined using qPCR, following the protocol described above. The qPCR analysis experiment was conducted in triplicate, the relative expression levels of *MrTNF* were determined using the $2^{-\Delta\Delta CT}$ method [32], and the results were presented as mean ± SD. To determine differences among the experiments, the expression level of *MrTNF* between the *A. hydrophila*-challenged group and that of the 2X PBS (control group) at each time point was analyzed by Student's *t*-test and One-way analysis of variance (ANOVA) with Post Hoc Tukey test using IBM SPSS Statistics (Version 25). Statistically significant differences were identified at $p<0.05$.

To confirm the infection of *A. hydrophila*-challenged prawns, the *A. hydrophila*-injected prawns were randomly sampled. Each selected prawn was sampled for 10 μL of hemolymph and resuspended with 90 μL of sterile 2X PBS. The mixture was diluted to 10^{-3}- and 10^{-4}-fold dilutions. An aliquot of 100 μL of each dilution was spread onto a TSA plate and incubated plate at 37°C overnight for colony counting. The single bacterial colony was picked for colony PCR amplification using Platinum® *Taq* DNA Polymerase

(Invitrogen, USA) with specific primers, AHH1F and AHH1R (Table 1), and the PCR conditions as described above.

Immune challenge with MrNV

Similar to the *A. hydrophila* challenge experiment, we conducted the *Mr*NV challenge experiment based on the mortality period of the *Mr*NV-infected prawn [37]. We collected the prawn samples every day for seven days, and the experiment was performed according to our previous studies study [29, 38]. The healthy *M. rosenbergii* (1-2 g body weight) were divided into two groups, each comprising 24 individual prawns in a 100-liter plastic tank. The first group was intramuscularly injected at the third abdominal segment using a 1 mL syringe (0.33 x 13 mm) with 50 μL of *Mr*NV (8.05×10^{11} copies/μL nucleic acids) as the challenged group. The control group was injected with 50 μL of sterile TN buffer. Target organs including gills, hepatopancreas, and muscle, were collected from each group (3 prawns per time point) at 0, 1, 2, 3, 4, 5, 6, and 7 days post-injection.

The expression of *MrTNF* was determined using qPCR, following the same protocol as described above. The qPCR analysis experiment was conducted in triplicate, the relative expression levels of *MrTNF* were determined using the $2^{-\Delta\Delta CT}$ method [32], and the results were presented as mean $\pm$ SD. To determine differences among the experiments, the expression of *MrTNF* between the challenge and control groups at each time point was analyzed by Student's *t*-test and One-way analysis of variance (ANOVA) with Post Hoc Tukey test using IBM SPSS Statistics (Version 25). Statistically significant differences were identified at $p < 0.05$.

To quantify the *Mr*NV copy number in the prawns, viral nucleic acids were extracted from muscle tissues at each time point using the High Pure Viral Nucleic Acid Kit (Roche, Switzerland) following the manufacturer's protocol. The concentration of total RNA was measured using a NanoDrop Lite Spectrophotometer (Thermo Fisher Scientific, USA), and 2 μg of total RNA served as a template for cDNA synthesis using a first-strand cDNA synthesis kit (Invitrogen, USA). The resulting total cDNA (200 ng/μL) was then used as a template for determining the viral copy numbers of *Mr*NV through qPCR, employing specific primers, RNA1_RP (Table 1), and *Taq*Man probe (FAM-ACCCTTCGACCCCAGCAATGGTG-TAMRA). The qPCR was performed using SensiFAST Probe No-ROX Kit (BioLine, UK) under the following conditions: 1 cycle at 94 °C for 5 mins; 50 cycles at 94 °C for 30 s, and 58°C for 30 s, as previously described method [29].

Molecular docking analysis

To predict the protein structure of *Mr*TNF, the deep learning technology AlphaFold2 (AF2) was used to generate the three-dimensional (3D) structure model [39]. The algorithm was executed using the resources of Google Colaboratory (Colab) [40]. The predicted protein structure of *Mr*TNF was optimized within the surrounding solvent environment by Molecular dynamics (MD) simulations. MD simulations were conducted using the GROMACS 2023.2 software package [41, 42], employing force field parameters with AMBER14SB [43] for the protein solvating the systems in an octahedral box with the TIP3P water model. The protonation states of *Mr*TNF were carried out under specific conditions at pH 7.5 using the Adaptive

Poisson–Boltzmann Solver (APBS) software [44]. To neutralize the systems, Sodium ions (Na$^+$) were added to counterbalance the negative charge. To obtain the Gibbs free energy landscape, MD simulations were carried out at a temperature of 301 K and a pressure of 1 bar. To minimize energy, 50,000 steps were performed, followed by a 1-nanosecond (ns) equilibration of the entire system, and continued for a duration of 600 ns. Post-simulation, the global minimum structures were calculated from the Gibbs free energy landscape for the protein-protein binding affinities analysis. The protein-protein docking of the *Mr*TNF and Protruding (P)-domain of *Mr*NV (PDB ID: 5YKV) complex was performed using the ClusPro web server [45].

Results

Cloning the full-length cDNA of MrTNF and sequence analysis

The tumor necrosis factor gene of *M. rosenbergii*, designated as *MrTNF*, was cloned and isolated using RACE. We confirmed the identification of *Mr*TNF through BLASTp, which revealed the highest identity with *Mn*TNF from *M. nipponense*, at 91.88%. The full-length *MrTNF* was 1830 bp, which consisted of a 5′ untranslated region (5′-UTR) of 396 bp and 3′-UTR of 54 bp. The open reading frame (ORF) was 1380 bp and encoded 459 amino acid residues, with a molecular mass of 51.3 kDa and an isoelectric point of 9.21. However, no polyadenylation signal was at the 3′ end (Figure 1). Analysis of the *Mr*TNF protein revealed the presence of an N-terminus transmembrane domain at amino acid positions 21-43 and a C-terminus TNF homology domain (THD) at positions 324-446 (Figure 2). A pairwise alignment of *Mr*TNF demonstrated significant conservation with crustacean TNFs, showing a similarity score of 93.39% with *Mn*TNF and 54.28% with *Es*TNFSF, representing the highest and lowest similarity, respectively (Figure 3). The multiple sequence alignment of TNFs revealed the presence of two conserved cysteine residues within the TNF homology domain (THD) (Figure 4). The full-length cDNA of *MrTNF* was submitted to the NCBI GenBank database under the accession number MW590714.

```
1     TGCGTGTGTGCGTGGTCCAGTGCATAAAAGCGTGGCGCAGGGATCTTGCTGGGTAGTGCCGTTCGTGGCAGCCGAGTAGAAGGTAACATT   90
91    CGTGCCCAGTCTCTGCACCCTCGCGTCTAACACGTTGGCTTCACTCTCCCGACCGACACGTGGGGCTCCCGGCGTCCGGACAGAGATAAA   180
181   CCGCGAGAGATCTGAGCAGTCACCTCCGAGAGGGAGGCTGAGTTTTTCCAGAGGCGTTCTTTCTGATTAAAAACTTCAAGCACGCTTTTA   270
271   AAAGACTTCCAGGCGCTGTCATTGCAATTCATTATCTGAGCCGTATAGCTTGGAGGGTTTTGGAGTGAACGCCCTCCCTTGTACACAATA   360

361   CTTCCAGCCTCAGCAGCGCCTTCGATCGTCGCAGAC̲A̲T̲G̲GAAAAGACGCCCATGTACGCTGTGGTGACGCCCTCCGGCCCCAAGAAGTCC   450
1                                        M̲  E  K  T  P  M  Y  A  V  V  T  P  S  G  P  K  K  S     18

451   CGCCGGGTGATATGGGTGGGCTCTGGCCGTCAGCTTGGTCGTCTCATAATCGCGGGCGTGACAGGTTACGTGGAGAAGCGCCAGATCGAC   540
19     R  R  *V  I  W  V  G  S  G  R  Q  L  G  R  L  I  I  A  G  V  T  G  Y  V  E*  K  R  Q  I  D    48

541   CGAGTGAACGCCCTCGAAGAGACCGTCCTGCAGATGCAGCTCCACATGGAGCAACTCCTCCAGTTCACTCACGAGTACCTCGAGTACGAG   630
49     R  V  N  A  L  E  E  T  V  L  Q  M  Q  L  H  M  E  Q  L  L  Q  F  T  H  E  Y  L  E  Y  E     78

631   GAGGAGGAGGACCTCGACAATCCTCAGGGCGTCTATGAGGAGCTGACAGTGAGGGGCGTGGTGAGGAAGAAACGACAAGCCCCCAGCGAC   720
79     E  E  E  D  L  D  N  P  Q  G  V  Y  E  E  L  T  V  R  G  V  V  R  K  K  R  Q  A  P  S  D    108

721   GACAGCGACAAGAGCGGCGGAGTTCCCATATATGAGGAAGCATATGGAGTCAACCTTAATAATCGTTTCAATTCCGAGGGTCTTCGCCTC   810
109    D  S  D  K  S  G  G  V  P  I  Y  E  E  A  Y  G  V  N  L  N  N  R  F  N  S  E  G  L  R  L    138

811   TACGAGTCGTTCGGAGACAGCCAAAGCAGCGACCAGCTCAACTTGGAAACGACCGAATCACCAATCAAACCTTACCACAGAGTTTCGAAC   900
139    Y  E  S  F  G  D  S  Q  S  S  D  Q  L  N  L  E  T  T  E  S  P  I  K  P  Y  H  R  V  S  N    168

901   TTGTGGGTCCCTAAGAAGAGACGCCAGCGGTACCCACCAGCTTCAGGCCCTGAACTCTCCCCCAGGGCTCAAGTCAAGGCAGTAGATGAC   990
169    L  W  V  P  K  K  R  R  Q  R  Y  P  P  A  S  G  P  E  L  S  P  R  A  Q  V  K  A  V  D  D    198

991   GACAGCAGCGACTACGAAGACTACGACGCAGAGAACGTCGCTCTCACTCGACAGGGAAGTGGAAGACGCCGATCTCCGGTCCTTCAGAGG   1080
199    D  S  S  D  Y  E  D  Y  D  A  E  N  V  A  L  T  R  Q  G  S  G  R  R  R  S  P  V  L  Q  R    228

1081  AGCATCCGCGTCAAGGCCACAGCCCGCAACGACGGATTCCCCTCCACCGGCGTCAACAGCGTAGTGCCCCAAACCTCAGCGGCCATCGTG   1170
229    S  I  R  V  K  A  T  A  R  N  D  G  F  P  S  T  G  V  N  S  V  V  P  Q  T  S  A  A  I  V    258

1171  GTCCCACAGACGCCAACAGTCGTCCGGCAAGGACCCCAGTCCTTCAAAGCCGCCGATGCTCTCGTTAACCCTTACGCTGGGAAGGATGCC   1260
259    V  P  Q  T  P  T  V  V  R  Q  G  P  Q  S  F  K  A  A  D  A  L  V  N  P  Y  A  G  K  D  A    288

1261  AGGAAGAAGAGGCCTAGGAAGAAGTCCTCACGCCGTGGGGACCGCAGACGAGGAGCCAGGTCAGCCATCACCCTGGGACATTTCGTGGCC   1350
289    R  K  K  R  P  R  K  K  S  S  R  R  G  D  R  R  R  G  A  R  S  A  I  T  L  G  H  F  V  A    318

1351  GCTCCTGCTAACCGGACCGCGCACCATGTATCTGGCAGCGACATTCACGATGAATGGACCCCTGCCGCTTGGATGGACAATCTGGGATTG   1440
319    A  P  A  N  R  T̲  A̲  H̲  H̲  V̲  S̲  G̲  S̲  D̲  I̲  H̲  D̲  E̲  W̲  T̲  P̲  A̲  A̲  W̲  M̲  D̲  N̲  L̲  G̲  L̲    348

1441  AACAGAAAATATACTCTCAGAAGAGGACTGGTCACCGTCAAAGAGTCTGGTCTTTATTACCTCTATGCTCAGGTATTGTATGAGCAAGGA   1530
349    N̲  R̲  K̲  Y̲  T̲  L̲  R̲  R̲  G̲  L̲  V̲  T̲  V̲  K̲  E̲  S̲  G̲  L̲  Y̲  Y̲  L̲  Y̲  A̲  Q̲  V̲  L̲  Y̲  E̲  Q̲  G̲    378

1531  CGCTTCGGCACAGGTTTCCAGGTGATGGTCGACGGTATTCCAGTCATGGACTGTACGATGACACCATCACAACCGTCCAGCTCTTGTCAT   1620
379    R̲  F̲  G̲  T̲  G̲  F̲  Q̲  V̲  M̲  V̲  D̲  G̲  I̲  P̲  V̲  M̲  D̲  C̲  T̲  M̲  T̲  P̲  S̲  Q̲  P̲  S̲  S̲  C̲  H̲    408

1621  ACGTCTGGCACGACATACTTGCAAAGAAACGCCGCCGTGTCCATCCGCGACCGCGAGAGTCACATGAACACCGTCAGGAGAGAAGAGAAC   1710
409    T̲  S̲  G̲  T̲  T̲  Y̲  L̲  Q̲  R̲  N̲  A̲  A̲  V̲  S̲  I̲  R̲  D̲  R̲  E̲  S̲  H̲  M̲  N̲  T̲  V̲  R̲  R̲  E̲  E̲  N̲    438

1711  AGCTTCTTCGGTCTGATCAAGCTCATGGACGCTCCGGAATCAGCCGAGAAGCTGCTCTTGGGA**TGA**GCCGTCCCTTCCTTCCCGGCAAGT   1800
439    S̲  F̲  F̲  G̲  L̲  I̲  K̲  L̲  M  D  A  P  E  S  A  E  K  L  L  L  G  *                          459

1801  CTTTGAAAAAAAAAAAAAAAAAAAAAAAAAAA   1830
```

Figure 1 The full-length cDNA of *MrTNF* and the deduced amino acid. The amino acid sequences in bold and italics indicated the transmembrane domain structure. The amino acid sequences in bold and underlined showed the TNF homology domain (THD) structure.
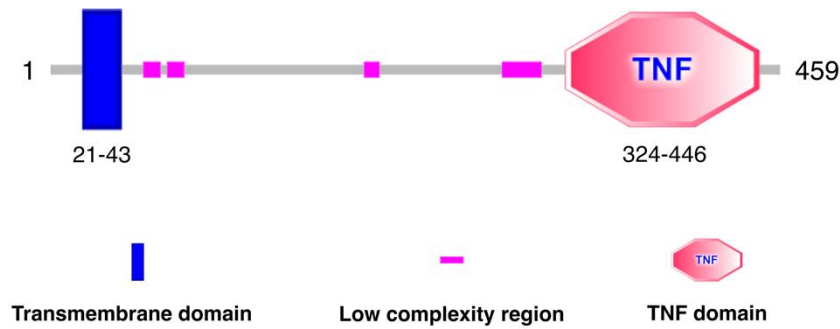
Figure 2 Schematic representation of the structural analysis of *Mr*TNF.

Figure 3 The pairwise alignment of *Mr*TNF and other TNFs. The pairwise similarity was shown in the upper right corner, and the pairwise identity was shown in the lower left corner. Accession numbers; *Macrobrachium rosenbergii* (*Mr*TNF, WDD44851), *Macrobrachium nipponense* (*Mn*TNF, QCS40507), *Marsupenaeus japonicus* (*Mj*TNF, BAJ10320), *Litopenaeus vannamei* (*Lv*EDA, XP_027209569.1; *Lv*TNFSF, AEK86525), *Eriocheir sinensis* (*Es*TNFSF, UYL04284), *Drosophila melanogaster* (*Dm*Eiger, NP_724878).
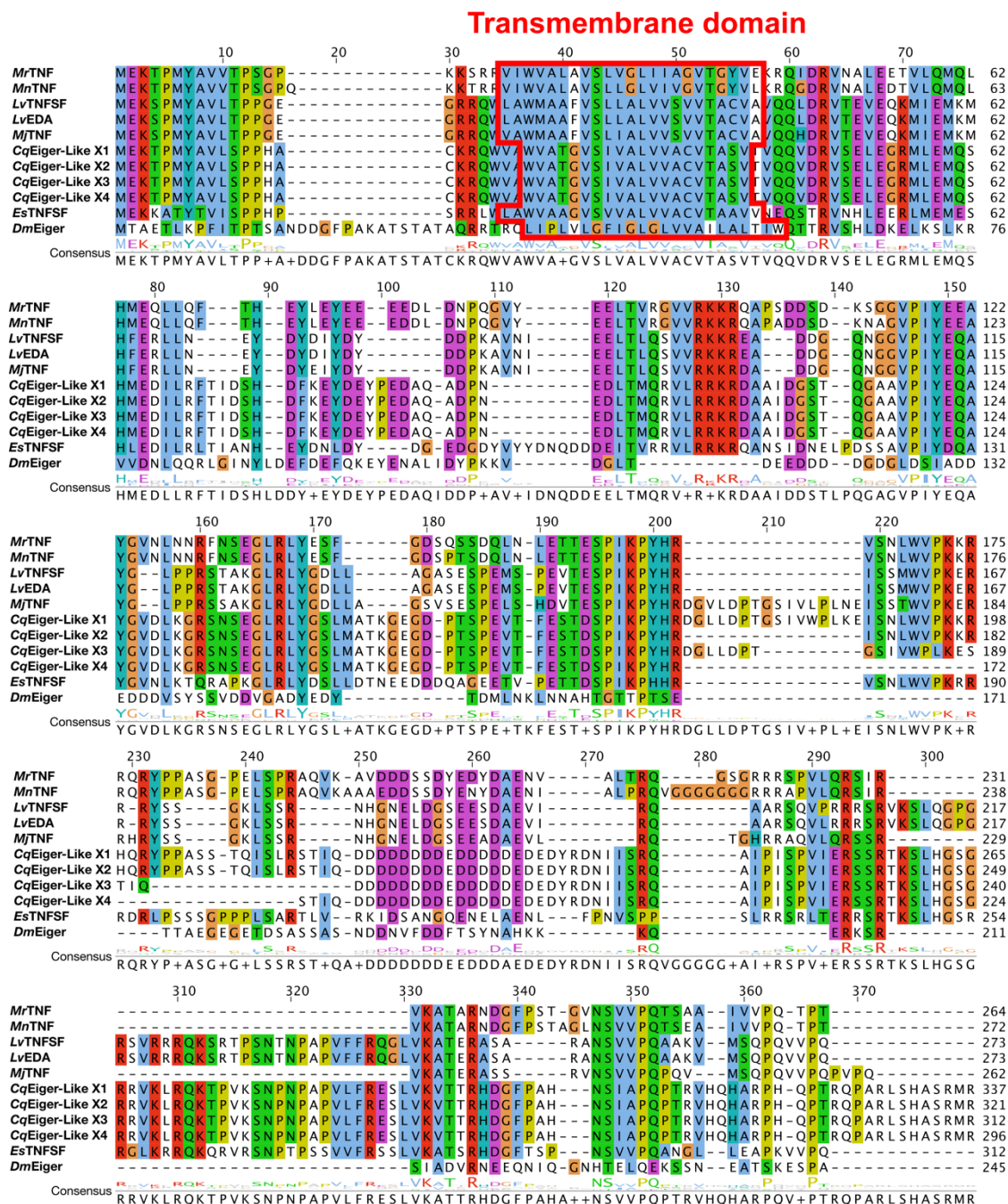
Figure 4 The multiple sequence alignment of amino acid sequences involving *Mr*TNF and other TNFs. The transmembrane domain was delineated with a red box, and the TNF domain was enclosed within a blue box. Notably, conserved cysteines (Cys) within the TNF domain were highlighted with a pink shading and marked with a red arrow. The identical or highly conserved residues were presented in similar shaded colors. Accession numbers; *Macrobrachium rosenbergii* (*Mr*TNF, WDD44851), *Macrobrachium nipponense* (*Mn*TNF, QCS40507), *Marsupenaeus japonicus* (*Mj*TNF, BAJ10320), *Litopenaeus vannamei* (*Lv*EDA, XP_027209569; *Lv*TNFSF, AEK86525), *Cherax quadricarinatus* (*Cq*Eiger-Like X1, XP_053644226; *Cq*Eiger-Like X2, XP_053644227; *Cq*Eiger-Like X3, XP_053644229; *Cq*Eiger-Like X4, XP_053644230), *Eriocheir sinensis* (*Es*TNFSF, UYL04284), and *Drosophila melanogaster* (*Dm*Eiger, NP_724878).
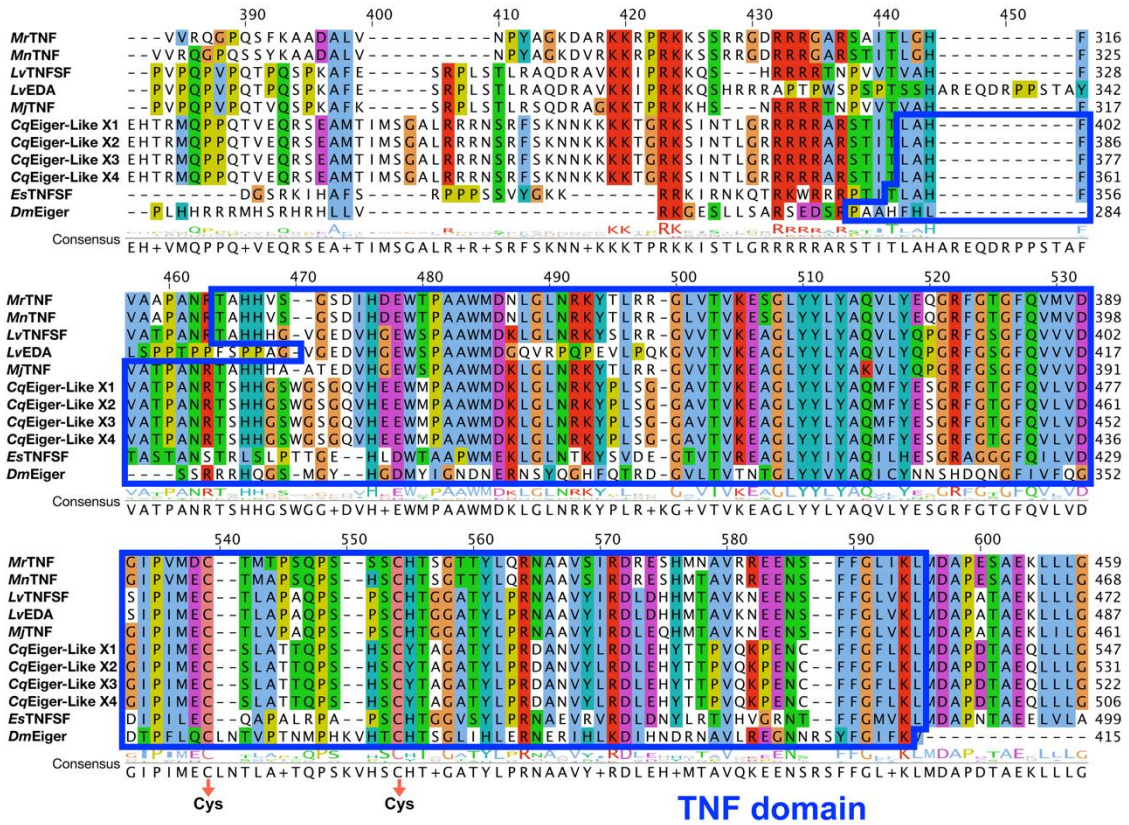
Figure 4 (Continue).

Phylogenetic tree

The conserved TNF homology domain (THD) from diverse species was aligned and used to reconstruct a phylogenetic tree. The result indicated that *Mr*TNF was closely related to *Mn*TNF from *M. nipponense* and clustered together with other TNFSF of crustaceans and insects (Figure 5).
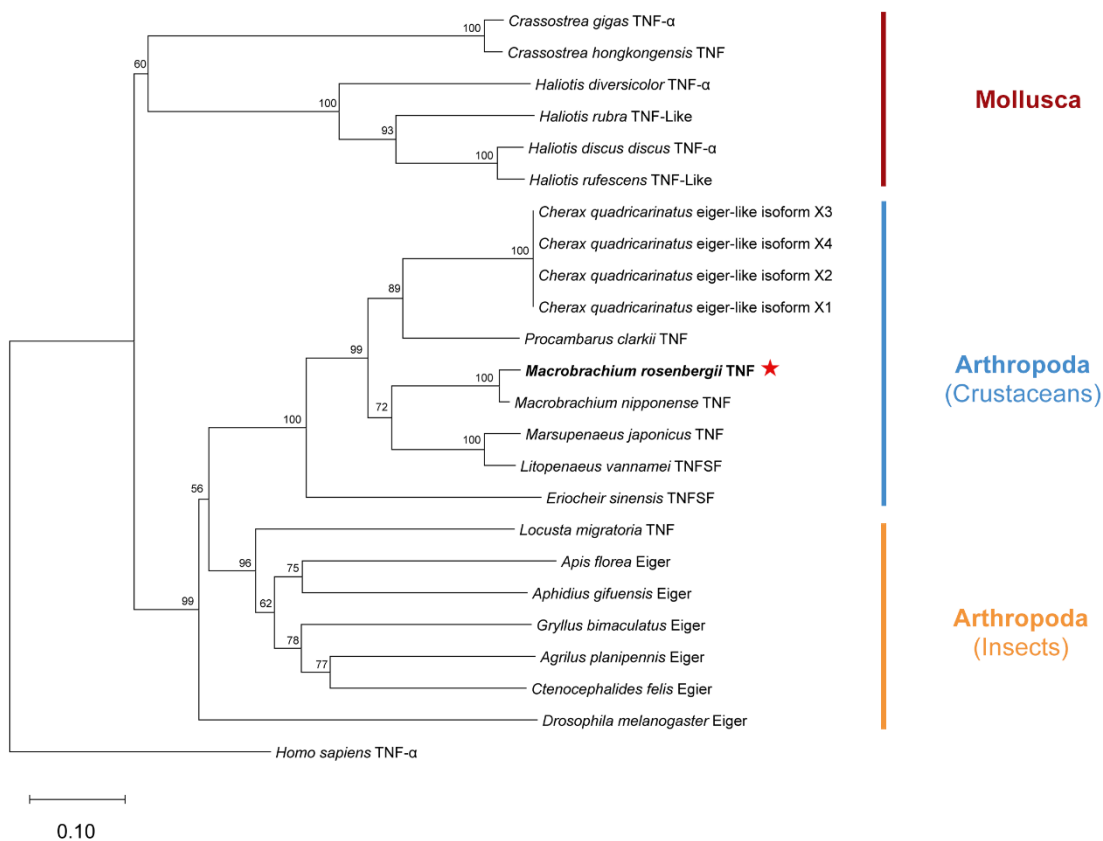

Figure 5 The phylogenetic tree analysis of TNF homology domain（THD）from various TNFSF members using the NJ method with bootstrap of 1000. The number above each clade indicates bootstrap statistics of the NJ phylogeny. Accession numbers; *Macrobrachium rosenbergii*（WDD44851）, *Macrobrachium nipponense*（QCS40507）, *Marsupenaeus japonicus*（BAJ10320）, *Litopenaeus vannamei*（AEK86525）, *Procambarus clarkia*（AYD41594）, *Cherax quadricarinatus*（Eiger-Like isoform X1, XP_053644226; Eiger-Like isoform X2, XP_053644227; Eiger-Like isoform X3, XP_053644229; Eiger-Like isoform X4, XP_053644230）, *Eriocheir sinensis*（UYL04284）, *Drosophila melanogaster*（NP_724878）, *Haliotis discus discus* (ACF75368), *Haliotis rubra* (XP_046566378), *Haliotis diversicolor* (ADP24261), *Haliotis rufescens* (XP_046345282), *Crassostrea gigas* (XP_011450585), *Crassostrea hongkongensis* (APC65296), *Locusta migratoria* (AKJ77887), *Gryllus bimaculatus* (GLH15015), *Aphidius gifuensis* (XP_044006453), *Agrilus planipennis* (XP_025837416), *Ctenocephalides felis* (XP_026470323), *Apis florea* (XP_012339578) *Drosophila melanogaster* (NP_724878), and *Homo sapiens* (NP_000585).

Tissue distribution of MrTNF in healthy prawns

   The expression of the *MrTNF* gene in healthy adult *M. rosenbergii* was examined in several tissues using qPCR. The relative expression of *MrTNF* was normalized with EF1α as a housekeeping gene. The study reveals that *MrTNF* expression can be stratified into three groups based on statistically significant differences at *p*<0.05. *MrTNF* mRNA was most highly expressed in the intestine, followed by moderate expression in muscle, stomach, and heart. In contrast, gills, hepatopancreas, and hemocytes constitute the group with the lowest expression (Figure 6).
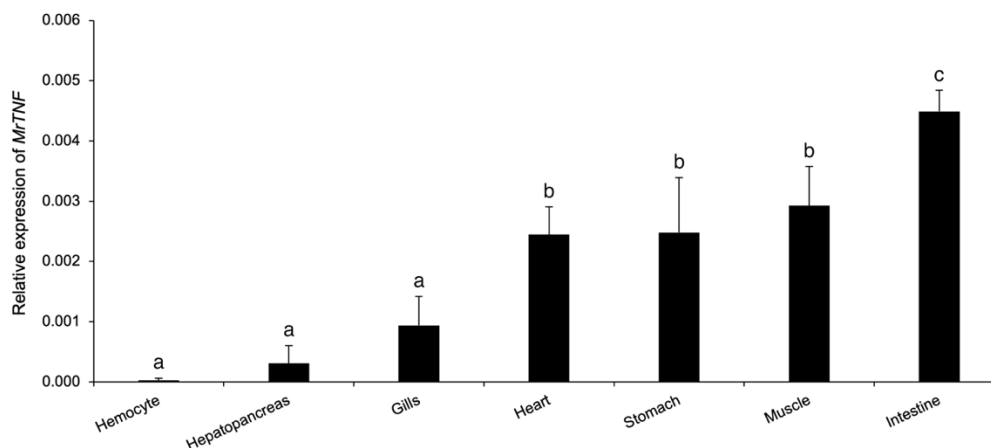

Figure 6 Tissue distribution of *MrTNF* gene in healthy prawns *Macrobrachium rosenbergii*. The relative expression of *MrTNF* was normalized by the expression of EF1α of each tissue with the result shown as the mean ± SD (*n*=3). Bars with different alphabets denoted significant differences at *p*<0.05.

The expression level of MrTNF in A. hydrophila-challenged prawns.

   The investigation involved exploring the role of *MrTNF* in the innate immune system after an immune challenge with *A. hydrophila* across several organs, including hemocytes, muscles, intestines, and stomach. The results demonstrated that *MrTNF* expression in hemocytes was significantly up-regulated at 6 and 24 hours post-injection (hpi) (Figure 7a). In addition, *MrTNF* was significantly up-regulated in muscle tissues at 12 hpi but significantly down-regulated at 24 hpi and returning to basal level at 36 hpi onward (Figure 7b). The expression level of *MrTNF* in the intestine was significantly up-regulated at 3 to 24 hpi and slightly down-regulated to basal level after 36 to 48 hpi (Figure 7c). Moreover, the expression level of *MrTNF* in the stomach was significantly up-regulated at 24 and 36 hpi (Figure 7d). The infection of A.*hydrophila* in the challenged group was verified by colony counting and PCR amplification from the collected hemolymph. The bacterial counts of the challenged prawns at 3, 6, 12, 24, 36, and 48 hpi were 8.2×10^4, 7.8×10^4, 6×10^5, 1.2×10^5, 1.7×10^5, and 9.3×10^4 CFU/mL, respectively.
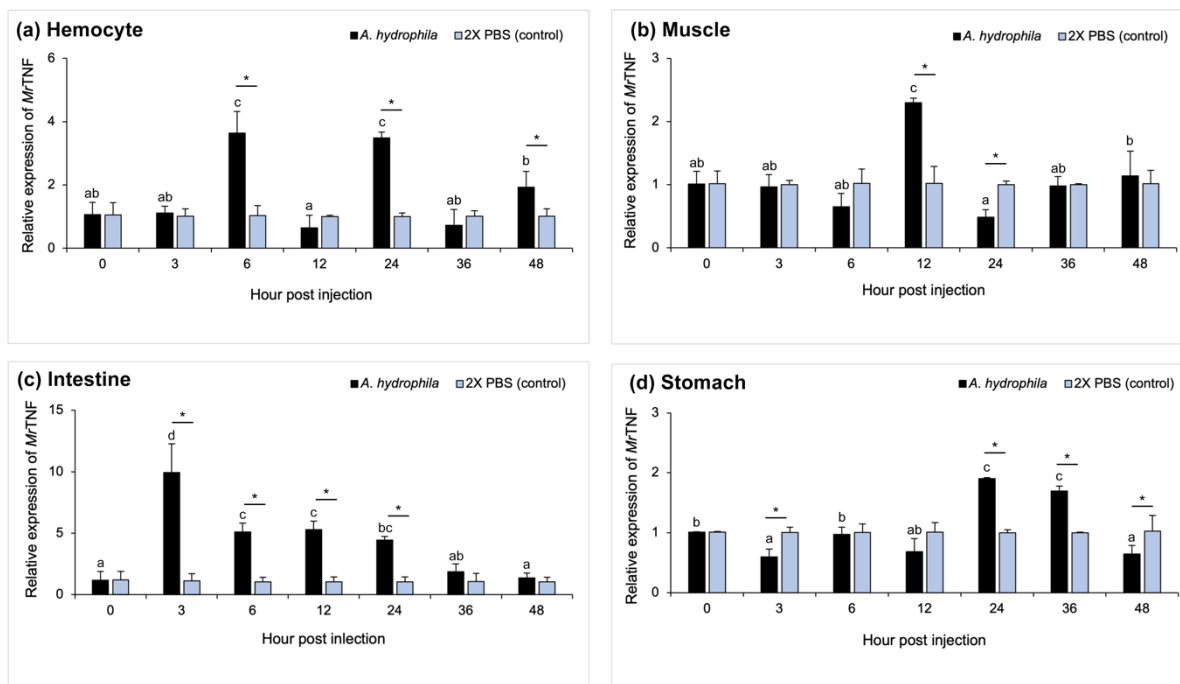
Figure 7 The expression level of *MrTNF* mRNA in hemocytes **(a)**, muscle **(b)**, intestine **(c)**, and stomach **(d)** after the immune challenge experiment with *Aeromonas hydrophila*. The relative expression of *MrTNF* was normalized by the expression of EF1α with results shown as the mean $\pm$ SD (*n*=3). Bars with different alphabets denoted the different expression levels between the *A. hydrophila* injection group at each time point. Asterisks indicated a significant difference at *p*<0.05 between the *A. hydrophila* group and the 2X PBS (control) group.

The expression level of MrTNF in MrNV challenged prawns

To examine the regulation of *MrTNF* expression in virus-infected, specifically in the muscle, gills, and hepatopancreas, a targeted immune challenge was conducted by injecting *Mr*NV. The results revealed that *MrTNF* expression level in muscle was significantly up-regulated at 2 days post-injection and significantly down-regulated at 3 to 7 days post-injection (Figure 8a). In gills, *MrTNF* expression was slightly up-regulated at 4 days post-injection and significantly up-regulated at 6 to 7 days post-injection (Figure 8b). *MrTNF* expression was significantly up-regulated in hepatopancreas at 3, 5, and 7 days post-injection (Figure 8c). The viral copy number of *Mr*NV at all tested time point were determined using qPCR analysis. The result revealed that the *Mr*NV copy numbers at 1-7days post-injection were 9.98×10^{11}, 5.51×10^{11}, 1.33×10^{12}, 1.02×10^{13}, 3.74×10^{14}, 2.32×10^{14} and 4.63×10^{11} copies/µL nucleic acids, respectively.
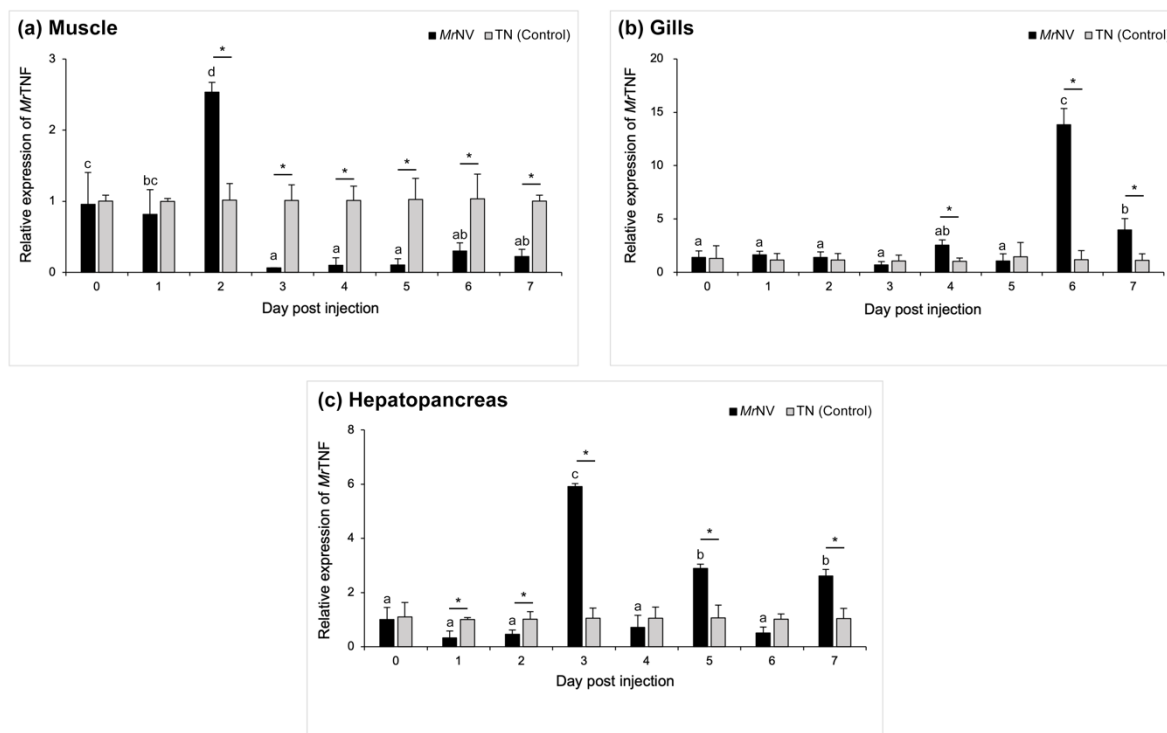
Figure 8 The expression level of *MrTNF* in muscle **(a)**, gills **(b)**, and hepatopancreas **(c)** after immune challenge with *Macrobrachium rosenbergii* nodavirus (*Mr*NV). The relative expression of *MrTNF* was normalized by the expression of EF1α with results shown as the mean $\pm$ SD (*n*=3). Bars with different alphabets denoted significant differences in the *Mr*NV injection group's expression level at each time point. Asterisks indicated a significant difference at *p*<0.05 between the *Mr*NV group and TN (control) group.

Protein structure prediction and protein-protein interaction analysis

The best models for the protein structure of *Mr*TNF were generated using the AF2 program, followed by the molecular dynamic simulation to identify the lowest energy state of the protein structure. The results from molecular dynamic simulation of *Mr*TNF were shown as the Gibbs free energy landscape contour maps (Figure 9a and Figure 9b). The bright yellow regions in these figures represent global minimum areas observed during the 584-600 ns periods, signifying the stability of the *MrTNF* protein structure, as shown in Figure 9c. Consequently, the structures corresponding to these intervals of the global energy minimum state were further utilized for studying protein-protein binding affinities. The predicted secondary structure of *Mr*TNF was composed of 13 α-helix and 8 β-sheets (Figure 9d).

The protein-protein interactions between *Mr*TNF and the P-domain protein of *Mr*NV were predicted using the ClusPro web server to identify the binding location and estimate the binding affinity. The docking results revealed the lowest binding free energy with a score of -971.25 kcal/mol, as presented in Table 2. These findings indicate that *Mr*TNF efficiently and stably binds to the P-domain protein of *Mr*NV. The binding location of *Mr*TNF with the P-domain protein (Figure 10a), and H-bond interactions within a 3 Å radius involve residues such as Glu25, Thr29, Thr31, Asp33, Glu55, Cys64, Ala69, Gly71, Ala80, Lys82, Tyr86, and Gln106 in chain A, as well as Val52, Ser53, Lys112, and Asp110 in chain B (Table 2 and Figure 10b).
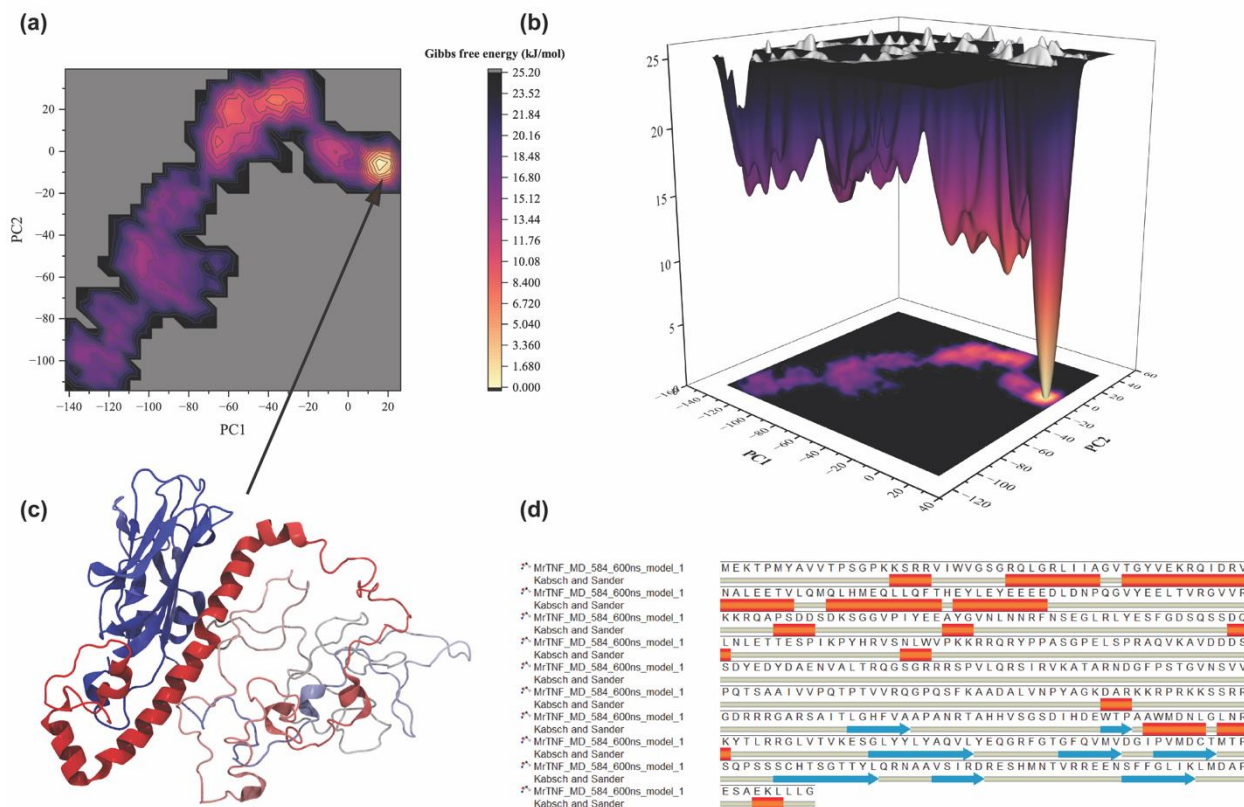
Figure 9 The contour maps depict the Gibbs free energy landscape of the *Mr*TNF protein of *Macrobrachium rosenbergii* in 2D structure **(a)** and 3D structure **(b)**, illustrating the protein structure at the global energy minimum state **(c)**. The predicted secondary structure of *Mr*TNF, the red box indicates the α-helix and the blue arrow indicates the β-sheet **(d)**.

Table 2 The binding interactions between MrTNF and the P-domain of *Mr*NV.

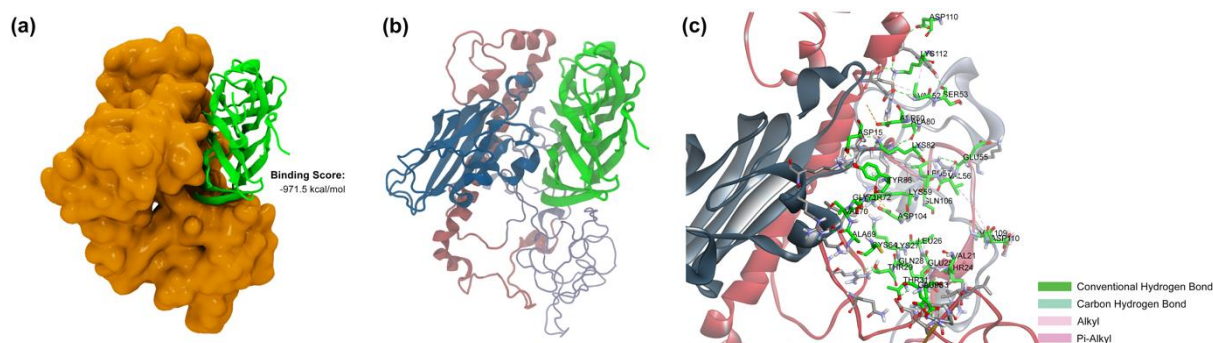| System	Binding energy (kcal/mol)	Domains	Surrounding amino acid within 3 Å	
			H-bond	**Hydrophobic**
***Mr*TNF− P domain**	-971.5	Chain A	Glu25, Thr29, Thr31, Asp33, Glu55, Cys64, Ala69, Gly71, Ala80, Lys82, Tyr86, Gln106	Val21, Leu26, Val56, Leu57, Lys82, Val109
		Chain B	Val52, Ser53, Lys112, Asp110	Val52, Lsy112

Figure 10 Illustrates the protein-protein conformations. *Mr*TNF and the P-domain are represented as orange and green, respectively **(a)**, the tertiary structure of *Mr*TNF (transparent) and the P-domain (green) **(b)**, along with the interaction locations within a 3 Å **(c)**.

Discussion

Tumor necrosis factor (TNF) is a cytokine belonging to the tumor necrosis factor superfamily (TNFSF) that plays a crucial role in cell inflammation, cell death, cell proliferation, and various functions in the immune system of living organisms [4]. In invertebrates, TNFSF was first discovered in fruit fly *Drosophila melanogaster*, known as Eiger, which was identified as a type II transmembrane protein with THD at the C-terminus, a transmembrane domain, and a cytoplasmic domain at the N-terminus [6]. The Eiger protein triggers insect cell death via the JNK pathway, involving the activation of Drosophila Nedd2-like caspase (DRONC) and Drosophila Apaf-1-related killer (DARK) enzymes, which are homologs of caspase-9 and apoptotic protease activating factor 1 (Apaf-1) in the TNF signaling pathway found in milk-feeding animals [46, 47].

TNFSF and TNFRSF were later identified by studying the transcriptome of the purple sea urchin *Strongylocentrotus purpuratus* [15]. Lipopolysaccharide-induced TNF-alpha factor (LITAF) was discovered in the oyster *Crassostrea gigas* (*Cg*-LITAF), a member of the TNFSF that stimulates the functions of transcription factors and cytokines in the innate immune system [11]. TNF was also found in the disk abalone *Haliotis discus discus* (*Ab*TNF-α), and it was shown to respond to invading pathogens such as bacteria and viruses [8]. TNFSF has been reported in four species of shrimp: *M. japonicus* (*Mj*TNF) [16]; *L. vannamei* (*Lv*TNFSF, *Lv*TNFRSF, and *Lv*LITAF) [17]; *P. clarkii* [18]; and *M. nipponense* (*Mn*TNF) [19].

This study presents the first report of the complete cDNA sequence of the tumor necrosis factor gene in the giant freshwater prawn *Macrobrachium rosenbergii* (*Mr*TNF). The *Mr*TNF protein contained a transmembrane domain and TNF homology domain (THD). Interestingly, *Mr*TNF exhibited structural similarity to *Mn*TNF, as both lacked a signal peptide [19]. Within the THD structure of *Mr*TNF, two conserved cysteine residues played a crucial role in signaling through the TNF receptor (TNFR), which contains cysteine-rich domains (CRD) for TNF binding [48]. The relationship between *Mr*TNF and TNFSF from other organisms was investigated by analyzing the THD structure. The phylogenetic tree analysis revealed that *Mr*TNF showed a close relationship with *Mn*TNF from *M. nipponense*. However, *Mr*TNF did not cluster with the TNFs of penaeid prawns, *M. japonicus*, and *L. vannamei*, as they formed a distinct subclade.

The difference between TNF in vertebrates and invertebrates is the types of cells that produce TNF. In vertebrates, TNF is produced by various immune cells, including, monocytes, dendritic cells, NK cells, macrophages, T cells, and B cells, in response to infection or other stimuli [2]. In invertebrates, TNF is mainly produced by hemocytes, the equivalent of white blood cells in vertebrates. Hemocytes are found in the circulatory system of invertebrates and are responsible for phagocytosis and other immune functions [49]. The expression levels of *MrTNF* were studied in various organs, with the highest expression found in the intestine, and high expression was observed in muscles, stomach, and heart but significantly lower expression in gills, hepatopancreas, and hemocytes. This expression pattern was similar to that of the *MjTNF* and *LvTNFSF* in which the TNF revealed high expression levels in muscle and stomach, but lower expression levels in the hepatopancreas and hemocytes [16, 17]. However, the *MnTNF* exhibited higher expression levels in the nerve cord and hemocytes, but lower expression in the hepatopancreas [19]. These findings suggest that the expression of the TNF gene may exhibit variability across different organisms.

The expanding body of evidence supports the understanding that TNFSF in crustaceans plays a significant role in the immune system, notably exhibiting varying patterns of expression levels in response to bacterial, fungal, and viral infections. The expression of *MrTNF* was enhanced in hemocytes, muscle, intestine, and stomach after challenges with *A. hydrophila*. In hemocytes, *MrTNF* expression level was up-regulated at 6 and 12 hpi after the *A. hydrophila* challenge, similar to the up-regulation of *EsTNFSF* expression level in hemocytes at 2, 6, 12, and 24 hpi after *Vibrio* challenge [21]. *MnTNF* expression level was up-regulated in gills at 6 hpi after *A. veronii* challenge [19]. Furthermore, the expression level of *MjTNF* in gills was up-regulated at 4 hpi with *V. penaeicida* stimulation and was up-regulated at 2 hpi with lipopolysaccharide (LPS) stimulation. *MjTNF* expression level was up-regulated in the lymphoid organ at 4h after peptidoglycan (PGN) stimulation and at 4 and 12h after poly I:C stimulation, but no significant difference in *MjTNF* expression level in LPS stimulated cells [16]. *LvTNFSF* expression was found to be up-regulated in gills, intestine, and hepatopancreas after the *S. aureus* challenge, but down-regulated in the intestine at 9 hpi with the *V. alginolyticus* challenge. *LvTNFSF* expression level was not changed in the intestine after challenge with *C. albicans*, but it was up-regulated in gills at 9 and 12 hpi and in hepatopancreas at 9 hpi [17]. The expression of *MrTNF* in the muscle was up-regulated at 12 hpi, correlating with the bacterial colony count in the hemolymph, indicating a significant peak at 12 hours after injection. Furthermore, the expression of *MrTNF* in the stomach was up-regulated at 24-36 hpi, corresponding to the bacterial colony count at 24-36 hours after injection, which remained high. In the virus-challenged experiment, the increase in *Mr*NV quantity on days 1-7 post-injection led to a response in the expression of *MrTNF* in various tissues, with changes observed in each tissue. Additionally, the expression level of *MrTNF* was found to be up-regulated in muscle on day 2, but significantly down-regulated on days 3, 4, 5, 6, and 7 after *Mr*NV challenge. These results were consistent with the down-regulation of *LvTNFSF* expression in the intestine at 3, 9, 12, and 24 hpi after the WSSV challenge, while *LvTNFSF* expression in gills and hepatopancreas was up-regulated after the WSSV challenge [17]. These comprehensive findings collectively suggest that crustacean TNF plays a crucial role in the immune response against various pathogen infections, showcasing distinctive expression patterns across multiple organs compared to the normal state of prawns in the control group. This suggests that *MrTNF* may serve as a significant component of the immune system, being triggered and activated to play

diverse roles in various organs during the immune response, particularly in response to Gram-negative bacterial and viral infections.

Many viruses have evolved strategies to evade the immune response by targeting the TNF signaling pathway. In mammals, poxviruses encode the cytokine response modifier (Crm) family, which includes homologs to viral TNF receptors (vTNFR) and viral TNF binding proteins (vTNFBP) [50, 51]. Crm proteins operate by binding to TNF and inhibiting its function in the immune response [52]. Ectromelia virus (ECTV) induces mousepox and carries the vTNFR gene known as CrmD. Wild-type and TNF deletion mice showed no detectable TNF expression during ECTV infection. In contrast, infection with a CrmD deletion mutant virus resulted in increased TNF secretion and inflammatory cytokine production [53]. These findings suggested the significant involvement of TNF in antiviral immunity. In this study, molecular docking analysis revealed that *Mr*TNF efficiently binds to the protruding (P)-domain of *Mr*NV. The P-domain, resembling a spike in structure, is involved in the host cell attachment [54, 55]. This discovery may provide supporting evidence correlating with *MrTNF* gene expression after *Mr*NV challenge. The expression of *MrTNF* in the muscle and hepatopancreas was down-regulated during day 3-7 post-injection, suggesting a response when the virus enters the cells. Moreover, the expression of *MrTNF* in the muscle, gills, and hepatopancreas was up-regulated after *Mr*NV injection, indicating an attempt to eliminate or prevent viral infection. These results suggest that *Mr*TNF interacts with *Mr*NV at the early stage of infection, triggering a response in the innate immune system of prawns after viral infection. This mechanism is expected to be a defense strategy of *MrTNF* against pathogen invasion.

In summary, this study has identified and characterized the tumor necrosis factor of *M. rosenbergii* (*MrTNF*) and provided novel insights into the expression pattern of *MrTNF* in various organs and its potential role in the immune response against bacterial and viral infections. The findings highlighted the importance of studying the immune system of crustaceans, which could facilitate the development of innovative therapeutic approaches for the prevention and treatment of diseases in aquaculture.

Acknowledgments

References

1. Holbrook J, Lara-Reyna S, Jarosz-Griffiths H, McDermott M. Tumour necrosis factor signalling in health and disease. F1000Res. 2019;8.

2. Croft M, Benedict CA, Ware CF. Clinical targeting of the TNF and TNFR superfamilies. Nat Rev Drug Discov. 2013;12(2):147-68.

3. Suo F, Zhou X, Setroikromo R, Quax WJ. Receptor specificity engineering of TNF superfamily ligands. Pharmaceutics. 2022;14(1):181.

4. Goetz FW, Planas JV, MacKenzie S. Tumor necrosis factors. Dev Comp Immunol. 2004;28(5):487-97.

5. Chu WM. Tumor necrosis factor. Cancer Lett. 2013;328(2):222-5.

6. Igaki T, Kanda H, Yamamoto-Goto Y, Kanuka H, Kuranaga E, Aigaki T, et al. Eiger, a TNF superfamily ligand that triggers the *Drosophila* JNK pathway. Embo J. 2002;21(12):3009-18.

7. Kauppila S, Maaty WS, Chen P, Tomar RS, Eby MT, Chapo J, et al. Eiger and its receptor, Wengen, comprise a TNF-like system in *Drosophila*. Oncogene. 2003;22(31):4860-7.

8. De Zoysa M, Jung S, Lee J. First molluscan TNF-alpha homologue of the TNF superfamily in disk abalone: molecular characterization and expression analysis. Fish Shellfish Immunol. 2009;26(4):625-31.

9. Sun Y, Zhou Z, Wang L, Yang C, Jianga S, Song L. The immunomodulation of a novel tumor necrosis factor (CgTNF-1) in oyster *Crassostrea gigas*. Dev Comp Immunol. 2014;45(2):291-9.

10. Zheng Y, Liu Z, Wang L, Li M, Zhang Y, Zong Y, et al. A novel tumor necrosis factor in the Pacific oyster *Crassostrea gigas* mediates the antibacterial response by triggering the synthesis of lysozyme and nitric oxide. Fish Shellfish Immunol. 2020;98:334-41.

11. Park EM, Kim YO, Nam BH, Kong HJ, Kim WJ, Lee SJ, et al. Cloning, characterization and expression analysis of the gene for a putative lipopolysaccharide-induced TNF-alpha factor of the Pacific oyster, *Crassostrea gigas*. Fish Shellfish Immunol. 2008;24(1):11-7.

12. Liu J, Liu Y, Liu Y, Guo X, Lü Z, Zhou X, et al. Molecular cloning, expression analysis and immune-related functional identification of tumor necrosis factor alpha (TNFα) in *Sepiella japonica* under bacteria stress. Fish Shellfish Immunol. 2023;132:108509.

13. Yu Y, Qiu L, Song L, Zhao J, Ni D, Zhang Y, et al. Molecular cloning and characterization of a putative lipopolysaccharide-induced TNF-alpha factor (LITAF) gene homologue from Zhikong scallop *Chlamys farreri*. Fish Shellfish Immunol. 2007;23(2):419-29.

14. Li L, Qiu L, Song L, Song X, Zhao J, Wang L, et al. First molluscan TNFR homologue in Zhikong scallop: molecular characterization and expression analysis. Fish Shellfish Immunol. 2009;27(5):625-32.

15. Hibino T, Loza-Coll M, Messier C, Majeske AJ, Cohen AH, Terwilliger DP, et al. The immune gene repertoire encoded in the purple sea urchin genome. Dev Biol. 2006;300(1):349-65.

16. Mekata T, Sudhakaran R, Okugawa S, Inada M, Kono T, Sakai M, et al. A novel gene of tumor necrosis factor ligand superfamily from kuruma shrimp, *Marsupenaeus japonicus*. Fish Shellfish Immunol. 2010;28(4):571-8.

17. Wang PH, Wan DH, Pang LR, Gu ZH, Qiu W, Weng SP, et al. Molecular cloning, characterization and expression analysis of the tumor necrosis factor (TNF) superfamily gene, TNF receptor superfamily gene and lipopolysaccharide-induced TNF-α factor (LITAF) gene from *Litopenaeus vannamei*. Dev Comp Immunol. 2012;36(1):39-50.

18. Calderón-Rosete G, González-Barrios JA, Lara-Lozano M, Piña-Leyva C, Rodríguez-Sosa L. Transcriptional identification of related proteins in the immune system of the crayfish *Procambarus clarkii*. High Throughput. 2018;7(3):26.

19. Qin N, Tang T, Liu X, Xie S, Liu F. Involvement of a TNF homologue in balancing the host immune system of *Macrobrachium nipponense*. Int J Biol Macromol. 2019;134:73-9.

20. Li S, Jia Z, Li X, Geng X, Sun J. Identification and expression analysis of lipopolysaccharide-induced TNF-alpha factor gene in Chinese mitten crab *Eriocheir sinensis*. Fish Shellfish Immunol. 2014;38(1):190-5.

21. Huang Y, Si Q, Du S, Du J, Ren Q. Molecular identification and functional analysis of a tumor necrosis factor superfamily gene from Chinese mitten crab (*Eriocheir sinensis*). Dev Comp Immunol. 2022;134:104456.

22. Farook MA, Mohamed HSM, Tariq N, Shariq KM, Ahmed IA, editors. Giant freshwater prawn, *Macrobrachium rosenbergii* (de Man 1879) : A review. Int J Res Anal Rev. 2019;6(1):571-84.

23. Chen KF, Tan WS, Ong LK, Abidin SAZ, Othman I, Tey BT, et al. The *Macrobrachium rosenbergii* nodavirus: a detailed review of structure, infectivity, host immunity, diagnosis and prevention. Rev Aquacult. 2021;13(4):2117-41.

24. Huang Y, Ren Q. Innate immune responses against viral pathogens in *Macrobrachium*. Dev Comp Immunol. 2021;117:103966.

25. Hooper C, Debnath PP, Stentiford GD, Bateman KS, Salin KR, Bass D. Diseases of the giant river prawn *Macrobrachium rosenbergii*: a review for a growing industry. Rev Aquacult. 2023;15(2):738-58.

26. Senapin S, Jaengsanong C, Phiwsaiya K, Prasertsri S, Laisutisan K, Chuchird N, et al. Infections of *Mr*NV (*Macrobrachium rosenbergii* nodavirus) in cultivated whiteleg shrimp *Penaeus vannamei* in Asia. Aquac. 2012;338-341:41-6.

27. Payattikul P, Longyant S, Sithigorngul P, Chaivisuthangkura P. Development of a PCR Assay based on a single-base pair substitution for the detection of *Aeromonas caviae* by targeting the gyrB gene. J Aquat Anim Health. 2015;27(3):164-71.

28. Wang G, Clark CG, Liu C, Pucknell C, Munro CK, Kruk TM, et al. Detection and characterization of the hemolysin genes in *Aeromonas hydrophila* and *Aeromonas sobria* by multiplex PCR. J Clin Microbiol. 2003;41(3):1048-54.

29. Srisuk C, Choolert C, Bendena WG, Longyant S, Sithigorngul P, Chaivisuthangkura P. Molecular isolation and expression analysis of hemocyanin isoform 2 of *Macrobrachium rosenbergii*. J Aquat Anim Health. 2022;34(4):208-20.

30. Zhang H, Wang J, Yuan J, Li L, Zhang J, Bonami JR, et al. Quantitative relationship of two viruses (MrNV and XSV) in white-tail disease of *Macrobrachium rosenbergii*. Dis Aquat Organ. 2006;71(1):11-7.

31. Pasookhush P, Hindmarch C, Sithigorngul P, Longyant S, Bendena WG, Chaivisuthangkura P. Transcriptomic analysis of *Macrobrachium rosenbergii* (giant fresh water prawn) post-larvae in response to *M. rosenbergii* nodavirus (MrNV) infection: de novo assembly and functional annotation. BMC Genomics. 2019;20(1):762.

32. Livak KJ, Schmittgen TD. Analysis of relative gene expression data using real-time quantitative PCR and the $2-\Delta\Delta CT$ method. Methods. 2001;25(4):402-8.

33. Abdolnabi S, Ina-Salwany MY, Daud HM, Mariana SD, Abdelhadi YM. Pathogenicity of *Aeromonas hydrophila* in giant freshwater prawn *Macrobrachium rosenbergii*, cultured in East Malaysia. Iran J Fish Sci. 2015;14(1):232-45.

34. Vaniksampanna A, Longyant S, Charoensapsri W, Sithigorngul P, Chaivisuthangkura P. Molecular isolation and characterization of a spätzle gene from *Macrobrachium rosenbergii*. Fish Shellfish Immunol. 2019;84:441-50.

35. Srisuk C, Longyant S, Senapin S, Sithigorngul P, Chaivisuthangkura P. Molecular cloning and characterization of a Toll receptor gene from *Macrobrachium rosenbergii*. Fish Shellfish Immunol. 2014;36(2):552-62.

36. Choolert C, Pasookhush P, Vaniksampanna A, Longyant S, Chaivisuthangkura P. A novel tumor necrosis factor receptor-associated factor 6 (TRAF6) gene from *Macrobrachium rosenbergii* involved in antibacterial defense against *Aeromonas hydrophila*. Fish Shellfish Immunol. 2023;140:108945.

37. Low CF, Md Yusoff MR, Kuppusamy G, Ahmad Nadzri NF. Molecular biology of *Macrobrachium rosenbergii* nodavirus infection in giant freshwater prawn. J Fish Dis. 2018;41(12):1771-81.

38. Pasookhush P, Vaniksampanna A, Sithigorngul P, Longyant S, Chaivisuthangkura P. Molecular isolation and characterization of translationally controlled tumor protein (TCTP) gene from *Macrobrachium rosenbergii*. Aquac Int. 2020;28(6):2173-90.

39. Jumper J, Evans R, Pritzel A, Green T, Figurnov M, Ronneberger O, et al. Highly accurate protein structure prediction with AlphaFold. Nature. 2021;596(7873):583-9.

40. Mirdita M, Schütze K, Moriwaki Y, Heo L, Ovchinnikov S, Steinegger M. ColabFold: making protein folding accessible to all. Nature Methods. 2022;19(6):679-82.

41. Weng Y, Pan C, Shen Z, Chen S, Xu L, Dong X, et al. Identification of Potential WSB1 Inhibitors by AlphaFold modeling, virtual screening, and molecular dynamics simulation studies. Evid-Based Complement Altern Med. 2022;2022:4629392.

42. Abraham MJ, Murtola T, Schulz R, Páll S, Smith JC, Hess B, et al. GROMACS: High performance molecular simulations through multi-level parallelism from laptops to supercomputers. SoftwareX. 2015;1-2:19-25.

43. Maier JA, Martinez C, Kasavajhala K, Wickstrom L, Hauser KE, Simmerling C. ff14SB: Improving the accuracy of protein side chain and backbone parameters from ff99SB. J Chem Theory Comput. 2015;11(8):3696-713.

44. Jurrus E, Engel D, Star K, Monson K, Brandi J, Felberg LE, et al. Improvements to the APBS biomolecular solvation software suite. Protein Sci. 2018;27(1):112-28.

45. Desta IT, Porter KA, Xia B, Kozakov D, Vajda S. Performance and its limits in rigid body protein-protein docking. Structure. 2020;28(9):1071-81.

46. Tang T, Li W, Wang X, Wu Y, Liu F. A house fly TNF ortholog Eiger regulates immune defense via cooperating with Toll and Imd pathways. Dev Comp Immunol. 2019;90:21-8.

47. Moreno E, Yan M, Basler K. Evolution of TNF signaling mechanisms: JNK-dependent apoptosis triggered by Eiger, the *Drosophila* homolog of the TNF superfamily. Curr Biol. 2002;12(14):1263-8.

48. Ware CF. The TNF superfamily. Cytokine Growth Factor Rev. 2003;14(3-4):181-4.

49. Jiravanichpaisal P, Lee BL, Söderhäll K. Cell-mediated immunity in arthropods: hematopoiesis, coagulation, melanization and opsonization. Immunobiology. 2006;211(4):213-36.

50. Rahman MM, McFadden G. Modulation of tumor necrosis factor by microbial pathogens. PLoS Pathog. 2006;2(2):e4.

51. Miranda FJA, Alonso-Sánchez I, Alcamí A, Hernaez B. TNF decoy receptors encoded by poxviruses. Pathogens. 2021;10(8).

52. Benedict CA. Viruses and the TNF-related cytokines, an evolving battle. Cytokine Growth Factor Rev. 2003;14(3-4):349-57.

53. Al Rumaih Z, Tuazon Kels MJ, Ng E, Pandey P, Pontejo SM, Alejo A, et al. Poxvirus-encoded TNF receptor homolog dampens inflammation and protects from uncontrolled lung pathology during respiratory infection. Proc Natl Acad Sci U S A. 2020;117(43):26885-94.

54. Ho KL, Gabrielsen M, Beh PL, Kueh CL, Thong QX, Streetley J, et al. Structure of the *Macrobrachium rosenbergii* nodavirus: a new genus within the Nodaviridae? PLoS Biol. 2018;16(10):e3000038.

55. Chong LC, Ganesan H, Yong CY, Tan WS, Ho KL. Expression, purification and characterization of the dimeric protruding domain of *Macrobrachium rosenbergii* nodavirus capsid protein expressed in *Escherichia coli*. PLoS One. 2019;14(2):e0211740.